Journal of Photochemistry and Photobiology B: Biology 129 (2013) 36–47

Contents lists available at ScienceDirect

Journal of Photochemistry and Photobiology B: Biology

journal homepage: www.elsevier.com/locate/jphotobiol

# Synthesis and biological studies of steroidal pyran based derivatives

Shamsuzzaman [a,*], Ayaz Mahmood Dar [a], Yusuf Khan [b], Aamir Sohail [c]

[a] Department of Chemistry, Aligarh Muslim University, Aligarh 202002, India
[b] International Centre for Genetic Engineering and Biotechnology, New Delhi 110067, India
[c] Department of Biochemistry, Aligarh Muslim University, Aligarh 202002, India

ARTICLE INFO

*Article history:*
Received 6 July 2013
Received in revised form 17 September 2013
Accepted 25 September 2013
Available online 8 October 2013

*Keywords:*
4H-Pyran
DNA binding
Gel electrophoresis
MTT assay
Comet assay

ABSTRACT

Steroid based cancer chemotherapeutic agents of the type 2′-amino-3′-cyanocholest-6-eno[5,7-de]4H-pyrans (**1c**–**3c**) have been synthesized and characterized by the various spectroscopic and analytical techniques. The DNA binding studies of compounds (**1c**–**3c**) with CT DNA were carried out by UV–vis and fluorescence spectroscopy and gel electrophoresis. The compounds (**1c**–**3c**) bind to DNA preferentially through electrostatic and hydrophobic interactions with $K_b$ values found to be $5.4 \times 10^3$, $2.3 \times 10^3$ $M^{-1}$ and $1.97 \times 10^3$ $M^{-1}$, respectively indicating the higher binding affinity of compound (**1c**) towards DNA. The molecular docking study suggested that the electrostatic interaction of compounds (**1c**–**3c**) in between the nucleotide base pairs is due to the presence of pyran moiety in steroid molecule. All the compounds (**1c**–**3c**) cleave supercoiled pBR322 DNA via hydrolytic pathway, as validated by T4 DNA ligase assay. The compounds (**1c**–**3c**) were screened for *in vitro* cytotoxicity against the cancer and non-cancer cells SW480, A549, HepG2, HeLa, MCF-7, HL-60, DU-145, NL-20, HPC and HPLF by MTT assay. The compounds (**1c**–**3c**) were tested for genotoxicity (comet assay) involving apoptotic degradation of DNA and was analyzed by agarose gel electrophoresis and visualized by ethidium bromide staining. The results revealed that compound (**1c**) has better prospectus to act as cancer chemotherapeutic candidate which warrants further *in vivo* anticancer investigations.



## 1. Introduction

Steroids are a class of important polycyclic compounds which exhibit diverse biological activities. Except for the naturally occurring substances, most of steroidal pharmaceuticals are semi-synthetic compounds [1]. Several steroidal derivatives have been investigated as new curative agents for cancers and other diseases. It is proved that a number of biologically important properties of modified steroids are dependent upon structural features of the steroid ring system or side chain so this chemical modification of the steroid provides a way to alter the functional groups and numerous structure–activity relationships have been established by such synthetic alterations [2].

Pyran derivatives are of considerable interest in industry as well as in academia owing to their potential biological and medicinal activities, such as analgesic, anticancer, anti-inflammatory, antibacterial and also serve as potential inhibitors of human Chk-1 kinase (Fig. 1) [3]. Furthermore, the applications of pyran derivatives are not only found in pharmaceutical ingredients and biological agrochemicals [4] but they also constitute a structural unit of number of natural products [5].

DNA cleaving agents have attracted extensive attention in the field of molecular biology due to their potential applications [6]. Under uncatalyzed physiological conditions, the phosphodiester bonds of DNA are extremely stable and the half life of DNA hydrolysis is estimated to be around 200 million years [7]. Some of the metal complexes have been widely investigated as efficient cleaving agents of nucleic acids [8] but the serious issues over their lability and toxicity restricted the practical usage of these compounds in pharmacy [9]. To overcome these limitations, Gobel and co-workers [10] put forward the concept of 'metal free cleaving agents' which are being applied to active phosphodiesters like 'nucleic acid mimic' and RNA.

Although various modifications of steroids have been tried including derivatization, cyclization, and heterocyclization, very few efforts have been made towards the efficient synthesis and the study of DNA binding, cleavage, cytotoxic and genotoxic activity of steroid based 4H-pyrans. So in continuation of our previous work [11] herein, we report the synthesis of new steroidal 4H-pyrans as metal free DNA binding agents. The presence of —NH and —CO groups in the molecules can cooperatively participate in the interaction with DNA via hydrogen bonding. A computer aided molecular docking study was carried out to validate the specific binding mode of the compounds. Furthermore, these compounds

* Corresponding author. Tel.: +91 9411003465.
*E-mail address:* shamsuzzaman9@gmail.com (Shamsuzzaman).

1011-1344/$ - see front matter © 2013 Elsevier B.V. All rights reserved.
http://dx.doi.org/10.1016/j.jphotobiol.2013.09.004

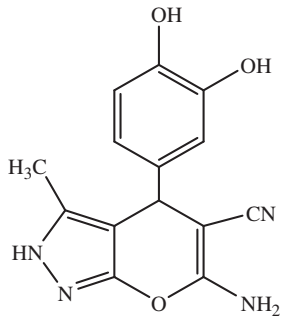


**Fig. 1.** Substituted pyran derivative-an inhibitor of human Chk-1 Kinase.

have also been screened for *in vitro* cytotoxicity against different human cancer and non-cancer cell lines.

## 2. Experimental

### 2.1. Materials and methods

All chemicals were purchased from Sigma–Aldrich (India) and Merck (India). Melting points were determined on a Kofler apparatus and are uncorrected. The IR spectra were recorded on KBr pellets with Perkin Elmer RXI Spectrometer and values are given in $cm^{-1}$. $^1H$ and $^{13}C$ NMR spectra were run in $CDCl_3$ on a JEOL Eclipse (400 MHz) instrument with TMS as internal standard and values are given in ppm ($\delta$). Mass spectra were recorded on a JEOL SX 102/DA-6000 Mass Spectrometer. Carbon, hydrogen and nitrogen contents were determined on Carlo Erba Analyzer Model 1106. Thin layer chromatography (TLC) plates were coated with silica gel G and exposed to iodine vapors to check the homogeneity as well as the progress of reaction. Sodium sulfate (anhydrous) was used as a drying agent. Super coiled pBR322 DNA was purchased from GeNei (India) and was used for the agarose gel experiment without further purification. Double-stranded calf thymus DNA, purchased from Sigma, was dissolved in a 0.1 M Tris-buffer. The purity of DNA was verified by monitoring the ratio of absorbance at 260 nm to that of 280 nm, which was in the range 1.8–1.9. The concentration of the DNA was determined spectrophotometrically using $\varepsilon_{260} = 6600\ M^{-1}\ cm^{-1}$ [12]. The human cancer cell lines used for the cytotoxicity experiment were SW480, A549, HepG2, HL-60, MCF-7, HeLa and DU-145 which were obtained from National Cancer Institute (NCI), biological testing branch, Federick Research and Development Centre, USA. The treated and control cancer cells were viewed with a FluoView FV1000 (Olympus, Tokyo, Japan) confocal laser scanning microscope (CLSM) equipped with argon and HeNe lasers. 2-Thiobarbituric acid (TBA) and trichloroacetic acid (TCA) were purchased from Merck (India). T4 DNA ligase enzyme was purchased from CalBioChem and was utilized as received.

### 2.2. Synthesis of cholest-5-ene derivatives (*1a*–*3a*)

3$\beta$-Acetoxycholest-5-ene (**1a**) was synthesized by heating mixture of cholesterol (25 mg), pyridine (37 mL freshly distilled over KOH) and freshly distilled acetic anhydride (25 mL) on a water bath for 2 h [13]. 3$\beta$-Chlorocholest-5-ene (**2a**) was synthesized by gently heating freshly purified thionyl chloride (10 mL) and cholesterol (12.5 g) on water bath for 1 h [14]. Cholest-5-ene (**3a**) was synthesized by dissolving 3$\beta$-chlorocholest-5-ene (5 g) in warm amyl alcohol (115 mL) and sodium metal (10 g) was added in small portions to the solution with continuous stirring over the period of 8 h [15].

### 2.3. General method for the synthesis of cholest-5-en-7-one derivatives (*1b*–*3b*)

A solution of *tert*-butyl chromate [*tert*-butyl alcohol (30 mL), $CrO_3$ (10 g), acetic acid (42 mL) and acetic anhydride (5 mL)] was added at 0 °C to a solution of cholest-5-ene derivatives (**1a**–**3a**) (4 g) in $CCl_4$ (75 mL), glacial acetic acid (15 mL) and acetic anhydride (5 mL) [15]. The contents were refluxed for 3 h and then diluted with water. The organic layer was washed with sodium bicarbonate solution (5%) and water and dried over anhydrous $Na_2SO_4$. Evaporation of solvents under reduced pressure provided oil which was crystallized from methanol to give cholest-5-en-7-one derivatives (**1b**–**3b**).

### 2.4. General method for the synthesis of steroidal 4H-pyran derivatives (*1c*–*3c*)

To a solution of cholest-5-en-7-one (**1b**–**3b**) (1 mmol) in absolute ethanol (20 mL) was added malononitrile in equimolar ratio followed by piperidine (1.5 mL). The reaction mixture was refluxed for 11 h. The progress of reaction was monitored by TLC. After completion of reaction, excess solvent was removed to three fourths of the original volume. The reaction mixture was taken in ether, washed with water and dried over anhydrous sodium sulfate. Evaporation of solvents and recrystallization from methanol afforded respective products (**1c**–**3c**) (see Scheme 1).

#### 2.4.1. 3β-Acetoxy-2′-amino-3′-cyanocholest-6-eno[5,7-de]4H-pyran (*1c*)

White powder, yield 70%, m.p. 163–164 °C; IR (KBr, $\nu_{max}/cm^{-1}$): 3340 ($NH_2$), 2203 (CN), 1713 ($OCOCH_3$), 1625, 1620 (C═C), 1065 (C—O), 1328 (C—N); $^1H$ NMR ($CDCl_3$, $\delta$, ppm): 5.69 (1H, s, $C_6$ *H*), 4.7 (1H, m, $C_3\alpha$-*H*, *W* ½ = 15 Hz), 2.5 (2H, brs, $NH_2$, exchangeable with $D_2O$), 2.05 (3H, s, $OCOCH_3$), 1.2 (3H, s, $C_{13}$-$CH_3$), 1.14 (3H, s, $C_{10}$-$CH_3$), 1.04 and 1.02 (other methyl protons); $^{13}C$ NMR ($CDCl_3$, $\delta$, ppm): 173.1 ($OCOCH_3$), 168 ($C_2'$), 157.2 ($C_7$), 132.2 (*C*N), 111.6 ($C_6$), 72.2 ($C_3$), 67.2 ($C_3'$); Anal. Calcd for $C_{32}H_{48}N_2O_3$%: C, 75.43, H, 9.26, N, 5.44. Found: C, 75.59, H, 9.44, N, 5.51. MS: *m*/*z* 508 [$M^{+\cdot}$].

#### 2.4.2. 3β-Chloro-2′-amino-3′-cyanocholest-6-eno[5,7-de]4H-pyran (*2c*)

Yellow powder, yield 80%, m.p. 143–144 °C; IR (KBr, $\nu_{max}/cm^{-1}$): 3396 ($NH_2$), 2259 (CN), 1630, 1625 (C═C), 1116 (C—O), 1327 (C—N), 742 (C-Cl); $^1H$ NMR ($CDCl_3$, $\delta$, ppm): 5.3 (1H, s, $C_6$ *H*), 3.9 (1H, m, $C_3\alpha$-*H*, *W* ½ = 17 Hz), 2.72 (2H, brs, $NH_2$, exchangeable with $D_2O$), 1.23 (3H, s, $C_{13}$-$CH_3$), 1.16 (3H, s, $C_{10}$-$CH_3$), 1.04 and 1.02 (other methyl protons); $^{13}C$ NMR ($CDCl_3$, $\delta$, ppm): 166 ($C_2'$), 155.2 ($C_7$), 129.2 (*C*N), 114.6 ($C_6$), 50.6 ($C_3'$), 50.2 ($C_3$). Anal. Calcd. for $C_{30}H_{45}ClN_2O$%: C, 74.26, H, 9.12, N, 5.61. Found: 74.38, H, 9.29, N, 5.78. MS: *m*/*z* 484/486 [$M^{+\cdot}$].

#### 2.4.3. 2′-Amino-3′-cyanocholest-6-eno[5,7-de]4H-pyran (*3c*)

White powder, yield 75%, m.p. 149–150 °C; IR (KBr, $\nu_{max}/cm^{-1}$): 3363 ($NH_2$), 2234 (CN), 1630, 1617 (C═C), 1078 (C—O), 1327 (C—N); $^1H$ NMR ($CDCl_3$, $\delta$, ppm): 5.26 (1H, s, $C_6$ *H*), 2.67 (2H, brs, $NH_2$, exchangeable with $D_2O$), 1.2 (3H, s, $C_{13}$-$CH_3$), 1.17 (3H, s, $C_{10}$-$CH_3$), 1.04 and 1.02 (other methyl protons); $^{13}C$ NMR ($CDCl_3$, $\delta$, ppm): 164 ($C_2'$), 154.3 ($C_7$), 134.4 (*C*N), 113.3 ($C_6$), 66.7 ($C_3$'), 23.2 ($C_3$); Anal. Calcd. for $C_{30}H_{46}N_2O$%: C, 79.96, H, 10.12, N, 6.17 found: C, 80.0, H, 10.22, N, 6.22; MS: *m*/*z* 450 [$M^{+\cdot}$].

### 2.5. DNA binding experiments

#### 2.5.1. Absorption and emission spectroscopy

The DNA binding experiments of compounds (**1c**–**3c**) were carried out by using absorption titration and emission spectroscopy

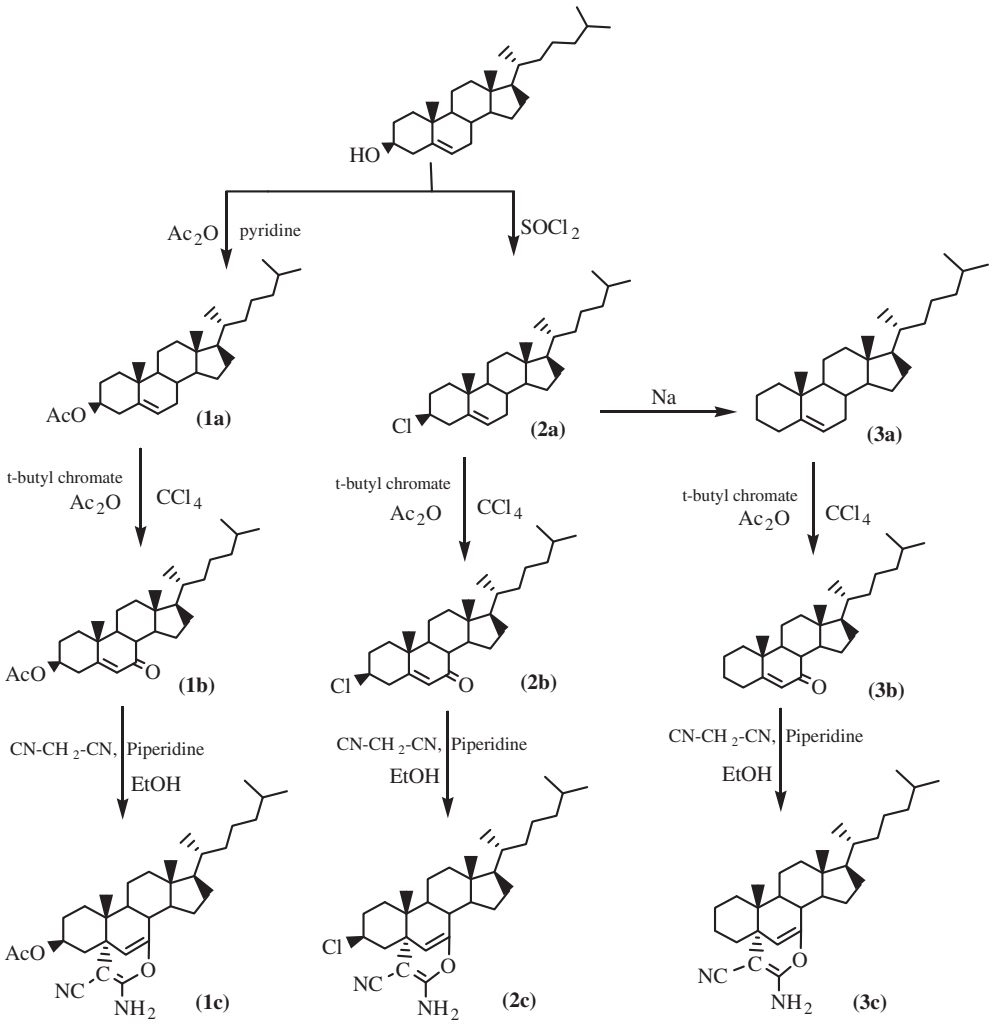


**Scheme 1.** Schematic pathway for the formation of steroidal 4H-pyran derivatives (**1c**–**3c**).

complies with the standard methods and practices [16–18]. To eliminate the absorbance of the DNA while measuring the absorption spectra, an equal amount of DNA was added to both the compound solution and the reference solution.

*2.5.2. Cleavage experiments*

Agarose gel electrophoresis [19] was used to carry out the cleavage experiments of supercoiled pBR322 DNA (300 ng) by compounds (**1c**–**3c**) (5–25 μM) in Tris-HCl/NaCl (5:50 mM) buffer at pH 7.2. The samples were incubated for 45 min at 310 K. A loading buffer containing 25% bromophenol blue, 0.25% xylene cyanol and 30% glycerol was added and electrophoresis was carried out at 50 V for 1 h in Tris–HCl buffer using 1% agarose gel containing 1.0 mg/mL ethidium bromide. Agarose gel electrophoresis was used to monitor the DNA cleavage with added reductant as in case of cleavage experiment without added reductant.

*2.5.3. Detection of hydroxyl radicals (·OH)*

The detection of hydroxyl radicals was investigated by the method studied by Quinlan and Gutteridge [20]. The reaction mixture (0.5 mL) containing Tris HCl (10 mM, pH 7.5), Calf thymus DNA (200 μg), increasing concentrations of compound **1c** and Cisplatin (12.5 μM, 25 μM, 50 μM, 75 μM, 100 μM, 200 μM, 400 μM, 600 μM), Cu (II) (100 μM) and volume was made up to 1 mL by buffer solutions and incubated for 60 min at 37 °C. Reaction was stopped using 0.5 mL of TCA (28%) and 0.5 mL of 1% TBA was added, boiled for 15 min and cooled to room temperature. The intensity was read at 532 nm.

*2.5.4. Relegation experiment with T4 DNA ligase enzyme*

To support the hydrolytic mechanism of DNA cleavage, the DNA relegation experiments were performed using T4 ligase enzyme by following the standard DNA relegation protocol [21]. The compounds (**1c**–**3c**) treated with pBR322 plasmid DNA (2 mg), ligation buffer of 1.5 mL in 10X, T4 ligase 1 mL (2 units) and 2.5 mL of $H_2O$ were mixed and incubated at 4 °C for 1 h. Subsequently, the samples were loaded on 1% agarose gel and visualized by staining with an ethidium bromide solution.

*2.5.5. Molecular docking*

The rigid molecular docking studies were performed using HEX 6.1 software [22]. The initial structure of the steroidal pyran **3c** was generated by Mercury modelling software. The molecules of compound were optimized for use in the following docking study. The crystal structure of the B-DNA dodecamer $d(CGCAAATTTCGC)_2$ (PDB ID: 1BNA) were downloaded from the protein data bank. All calculations were carried out on an Intel CORE i5, 2.6 GHz based machine running MS Windows 7 as the operating system.

Visualization of the docked pose have been done using PyMol molecular graphics program [23].

### 2.6. Anticancer activity

#### 2.6.1. Cell lines and culture conditions

Human cancer cell lines SW480 (colon adenocarcinoma cells), HeLa (cervical cancer cells), A549 (lung carcinoma cells), HepG2 (hepatic carcinoma cells), HL-60 (leukaemia), DU-145 (pancreatic cancer cells) and MCF-7 (breast cancer cells) were taken for the study. SW480, A549, HepG2, HL-60 and DU 145 cells were grown in RPMI 1640 [24] supplemented with 10% fetal bovine serum (FBS), 10U penicillin and 100 μg/mL streptomycin at 37 °C with 5% $CO_2$ in a humidified atmosphere. HeLa and MCF-7 cells were grown in Dulbecco's modified Eagle's medium (DMEM) [25] supplanted with FCS and antibiotics as described above for RPMI 1640. MCF10A immortalized breast cells were maintained in mammary epithelial basal medium supplemented with an MEGM mammary epithelial singlequot kit (Cambrex). NL-20 (normal lung cells), HPC (normal pulp cells) and HPLF (periodontal ligament fibroblasts) were grown at 37 °C with 5% $CO_2$, 95% air under the humidified conditions. Fresh medium was given every second day and on the day before the experiments were done. Cells were passaged at preconfluent densities, using a solution containing 0.05% trypsin and 0.5 mM EDTA.

*Cell viability assay (MTT).* The anticancer activity *in vitro* was measured using the MTT assay. The assay was carried out according to known protocol [26–28]. Exponentially growing cells were harvested and plated in 96-well plates at a concentration of $1 \times 10^4$ cells/well. After 24 h incubation at 37 °C under a humidified 5% $CO_2$ to allow cell attachment, the cells in the wells were respectively treated with target compounds at various concentrations for 48 h. The concentration of DMSO was always kept below 1.25%, which was found to be non-toxic to the cells. A solution of 3-(4,5-dimethylthizao1-2-y1)-2,5-diphenyltetrazolium bromide (MTT), was prepared at 5 mg/mL in phosphate buffered saline (PBS; 1.5 mM $KH_2PO_4$, 6.5 mM $Na_2HPO_4$, 137 mM NaCl, 2.7 mM KCl; pH 7.4). 20 μL of this solution were added to each well. After incubation for 4 h at 37 °C in a humidified incubator with 5% $CO_2$, the medium/MTT mixtures were removed and the formazan crystals formed by the mitochondrial dehydrogenase activity of vital cells were dissolved in 100 μL of DMSO per well. The absorbance of the wells was read with a microplate reader (Bio-Rad Instruments) at 570 nm. Effects of the drug cell viability were calculated using cells treated with DMSO as control. Cancer cells were grown on glass cover slips in 12-well cell culture plates (CoStar). After incubation with the test compound (**1c**), the disks were flipped on glass plates and the treated and control cancer cells were observed with a FluoView FV1000 (Olympus, Tokyo, Japan) confocal laser scanning microscope (CLSM) equipped with argon and HeNe lasers.

### 2.7. Data analysis

Cell survival was calculated using the formula: Survival (%) = [(absorbance of treated cells-absorbance of culture medium)/(absorbance of untreated cells − absorbance of culture medium)] × 100 [29,30]. The experiment was done in triplicate and the inhibitory concentration (IC) values were calculated from a dose response curve. $IC_{50}$ is the concentration in 'μM' required for 50% inhibition of cell growth as compared to that of control. $IC_{50}$ values were determined from the linear portion of the curve by calculating the concentration of agent that reduced absorbance in treated cells, compared to control cells, by 50%. Evaluation is based on mean values from three independent experiments, each comprising at least six microcultures per concentration level.

### 2.8. Comet assay (Single cell gel electrophoresis)

To assess the genotoxic effect of the steroidal 4H-pyrans (**1c–3c**), comet assay [31,32] was performed in MCF-7 cells. MCF-7 ($1 \times 10^6$) cells were treated with three different concentrations, 10, 25 and 50 μg/mL of steroidal 4*H*-pyrans (**1c–3c**) for 24 h. The cells were then washed and 200 μL of cell suspension in low melting agarose (LMA) was layered on to the labelled slides precoated with agarose (1.5%). The slides were placed on ice for 10 min and submerged in lysis buffer (2.5% NaCl, 100 mM EDTA, 10 mM Tris, 10% DMSO and 1% Troton X-100) at pH 10 at 4 °C for more than 1 h. The slides were then equilibrated in alkaline buffer (30 mM NaOH, 1 mM EDTA) at pH 13 at 4 °C, electrophoresed at 0.86 V/cm at 4 °C, neutralized, washed and dried. At the time of image capturing, the slides were stained with ethidium bromide (ETBr, 150 μL 1X) and cover slips were placed over them. For visualization of DNA-damage, ETBr-stained slides were observed under 209 objectives of a fluorescent microscope (Olympus BX-51, Japan). The images of 50–100 randomly selected cells were captured per slide using a CCD camera.

## 3. Results and discussion

### 3.1. Chemistry

Development of highly functional molecules from simple building blocks has always been the curiosity of synthetic chemists. We herein report the convenient synthesis of new steroidal 4*H*-pyran derivatives (**1c–3c**) by treatment of cholest-5en-7-one derivatives (**1b–3b**) with malononitrile in presence of piperidine in refluxing ethanol. The target compounds (**1c–3c**) were obtained in very good yields (70-80%). The mechanism for the formation of compounds (**1c–3c**) involves the Michael addition of active methylene reagent to the steroidal α, β-unsaturated ketone which on subsequent cyclization provided the desired products (Scheme 2) [33]. The stereochemical assignation of $C_5$-C bond has been made on the basis of two parameters, one is the half band width ($W_{1/2}$) values of $C_3$-axial proton in the $^1$H NMR spectra of **Ic** and **2c** which clearly suggested that A/B ring junction is *trans* [34]. Second is during the course of reaction, the attack of the reagent should be from the back (α) side which is less hindered and not from the front (β) side which is more hindered due to $C_{10}$ methyl group. Thus $C_5$-C bond should be axial (α) and *trans* to $C_{10}$ methyl group.

The characterization studies are in good agreement with proposed structures of steroidal pyrans. In the IR spectra, the absorption bands in the range 3340–3396 $cm^{-1}$ show the presence of $NH_2$ in the compounds (**1c–3c**) while as the absorption bands at 2203–2259 $cm^{-1}$ confirm the presence of CN in the compounds (**1c–3c**) attached to the pyran ring. The weak absorption band in the range 1625–1630 $cm^{-1}$ and 1617–1625 $cm^{-1}$ confirm the presence of two (C=C) in the compounds (**1c–3c**). In $^1$H NMR study, the broad singlet displayed at δ 2.5-2.72 integrating for two protons of =C—N*H*2 while as the presence of sharp singlet at δ 5.26–5.69 was assigned to olefinic proton (C6-*H*) in compounds (**1c–3c**). In $^{13}$C NMR study, the signals at δ 164–168, 154.3–157.2, 116–113, 50.2–67.2 confirm the presence of C2′, C7, C6, C3′, respectively in the products (**1c–3c**). The signals at δ 129–134 confirm the presence of *C*N in compounds (**1c–3c**). Finally the presence of distinct molecular ion peak [$M^{+\cdot}$] at *m*/*z*: 508, 484/486 and 450 in the MS also proved the formation of compounds (**1c–3c**).

### 3.2. DNA binding studies

#### 3.2.1. Electronic absorption titration

The covalent and/or non-covalent interactions are responsible for the binding of heterocyclic compounds with DNA. In covalent

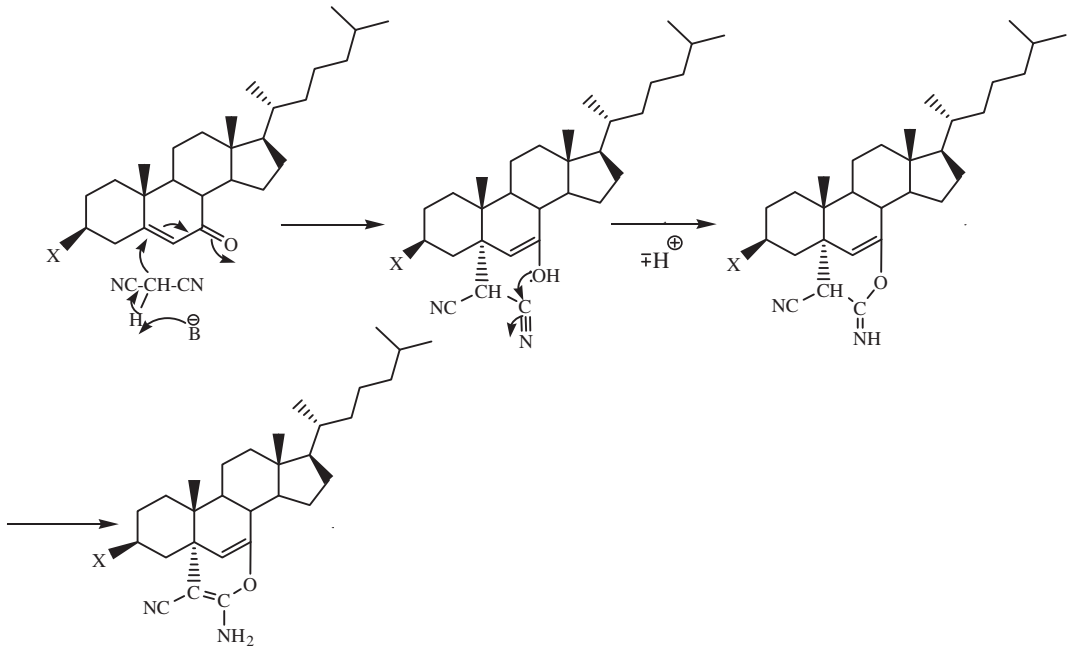


**Scheme 2.** Mechanistic pathway for the formation of steroidal 4H-pyran derivatives (**1c**–**3c**).

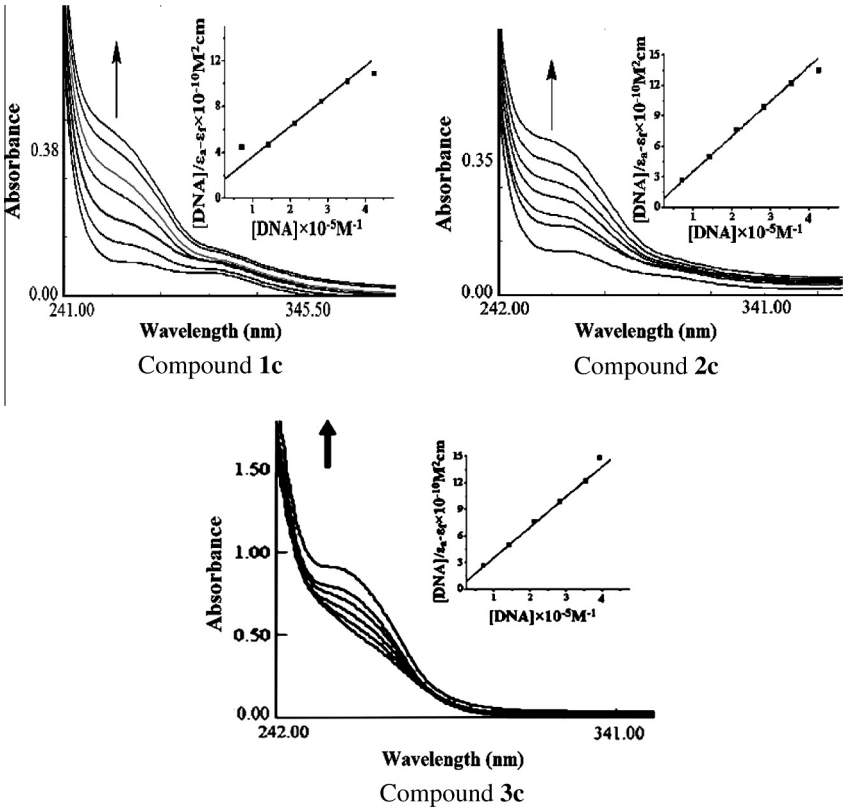


**Fig. 2.** Absorption spectra of steroid pyrans (**1c**–**3c**) in Tris-HCl buffer upon the addition of calf thymus DNA [compound] = $6.67 \times 10^{-6}$ M, [DNA] = $(0.70 - 4.24) \times 10^{-5}$ M. Arrow shows change in intensity with increasing concentration of DNA. Inset: plots of [DNA]/($\varepsilon_a - \varepsilon_f$) verses [DNA] for the titration of DNA with the compound.

binding, the easily leaving group of the compound is replaced by a nitrogen base of DNA such as guanine N7 while the non-covalent DNA interactions include electrostatic, intercalative and groove binding of heterocycles outside of a DNA helix. The absorption spectra of steroid pyrans (**1c**–**3c**) exhibited hyperchromism of 27.51%, 19.63% and 26.11%, respectively at intraligand absorption band (267–271 nm) as shown in Fig. 2. The observed hyperchromic effect revealed that compounds (**1c**–**3c**) bind to DNA electrostatically via non-covalent bonding with the DNA double helix. Moreover, steroid pyrans (**1c**–**3c**) exhibited a higher DNA binding profile due to the incorporation of $NH_2$ into the DNA binding grove. Since the hydrogen bonding interactions between —$NH_2$ groups of

steroidal pyran and the functional groups positioned on the edge of DNA bases feature novelty as it provides molecular recognition at the specific site at the cellular target. The intrinsic binding constant values ($K_b$) of the compounds were determined by monitoring the changes in the absorbance at the intraligand band with increasing concentration of CT DNA. In order to further compare the binding strength of the compounds, their intrinsic binding constant ($K_b$) were determined from the following equation:

$$[\mathrm{DNA}]/|\varepsilon_a - \varepsilon_f| = [\mathrm{DNA}]/|\varepsilon_b - \varepsilon_f| + 1/K_b|\varepsilon_b - \varepsilon_f| \quad (1)$$

where [DNA] represents the concentration of DNA, $\varepsilon_a$, $\varepsilon_f$ and $\varepsilon_b$ are the apparent extinction coefficients $A_{obs}/[M]$, the extinction coefficient for free compound and the extinction coefficient for compound in the fully bound form, respectively. In the plots of [DNA]/$\varepsilon_a - \varepsilon_f$ versus [DNA], $K_b$ is given by the ratio of the slope to the intercept.

The binding constants $K_b$ obtained for compounds (**1c**–**3c**) are $5.4 \times 10^3\ M^{-1}$, $2.3 \times 10^3\ M^{-1}$ and $1.97 \times 10^3\ M^{-1}$, respectively. Interestingly, the intrinsic binding $K_b$ value of compound **1c** is higher in magnitude than compound **2c** and **3c**. It may be due to the additional interaction like hydrogen bonding by the carbonyl moiety of acetate group ($OCOCH_3$) with DNA base pair which demonstrates the remarkably higher binding propensity of compound **1c** towards DNA.

### 3.2.2. Fluorescence spectral studies

An intense luminescence at 336 nm in 0.01 Tris–HCl/50 mM NaCl buffer was obtained in the emission spectra of compounds (**1c**–**3c**) at room temperature when excited at 269 nm. The emission intensity to a fixed amount of compounds gradually increases with no apparent change in the shape and position of the emission bands (shown in Fig. 3) on addition of increasing concentration of CT DNA ($0.70 \times 10^{-5}$ to $4.24 \times 10^{-5}$ M). The enhancement in emission intensity is related to the extent to which the compound penetrates into the hydrophobic environment inside the DNA helix therefore compound mobility is restricted at the binding site leading to a decrease in the vibrational mode of relaxation and thus avoids the quenching effect of the solvent molecules. The increase in the emission intensity revealed that the compound interacts by hydrophobic interaction in the DNA major groove.

To compare the binding affinity of compounds to DNA quantitatively, the binding constant '*K*' and binding site number '*n*' were calculated by using Scatchard equation (2) and (3).

$$C_F = C_T(F/F_o - P)(1 - P) \quad (2)$$

$$r/c = K(n - r) \quad (3)$$

where $C_F$ is the concentration of free compound, $C_T$ is the total concentration of compound; $F$ and $F_o$ are fluorescence intensities in the presence and absence of DNA, respectively. $P$ is the ratio of observed fluorescence quantum yield of the bound compound to that of the free compound. The value $P$ was obtained as the intercept by extrapolating from a plot of $F/F_o$ versus 1/[DNA], $r$ denotes the ratio of $C_B = (C_T - C_F)$ to the DNA concentration, '*c*' is the free compound concentration and '*n*' is the binding site number.

The binding constant determined from the Scatchard equation for compounds (**1c**–**3c**) was calculated to be $5.37 \times 10^3\ M^{-1}$, $2.51 \times 10^3\ M^{-1}$ and $2.2 \times 10^3\ M^{-1}$, respectively. The number of binding sites '*n*' for compounds (**1c**–**3c**) were found to be 1.36, 1.04 and 0.92, respectively indicating that compound **1c** has higher DNA binding propensity in agreement with the electronic absorption titration experiment.

### 3.2.3. Chemical nuclease activity

Heterocyclic compounds have played an important role in DNA endonucleolytic cleavage reactions. DNA cleavage is normally

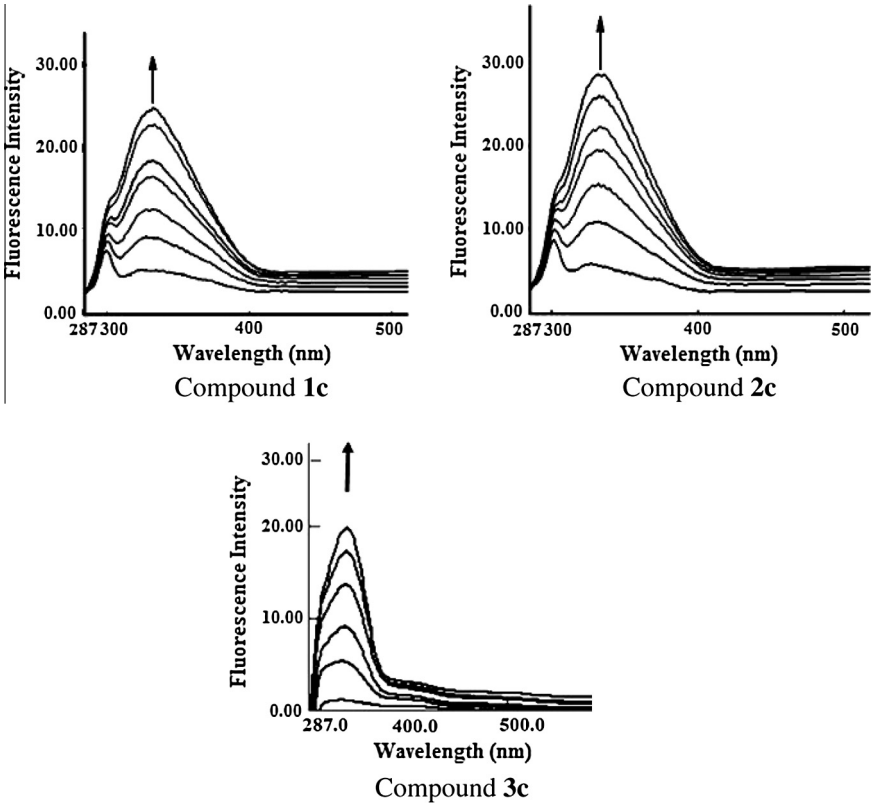


**Fig. 3.** Emission spectra of steroid pyrans (**1c**–**3c**) in Tris-HCl buffer (pH 7.2) in the presence and absence of CT DNA at room temperature. Arrow shows change in intensity with increasing concentration of DNA.

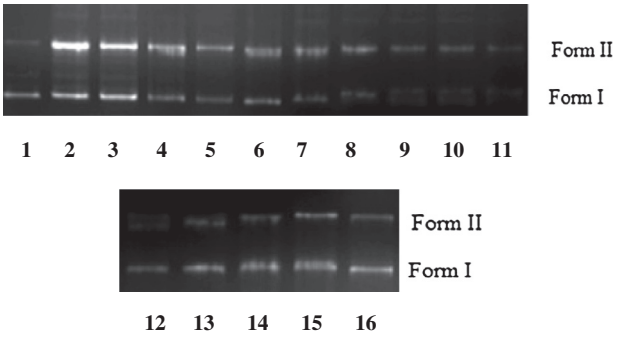


**Fig. 4.** Gel electrophoresis diagram showing cleavage of pBR322 supercoiled DNA (300 ng) by compounds (**1c–3c**) at 310 K after incubation for 1 h. Lane 1: DNA control; Lane 2: 5 μM of **1c** + DNA; Lane 3: 10 μM of **1c** + DNA; Lane 4: 15 μM of **1c** + DNA; Lane 5: 20 μM of **1c** + DNA; Lane 6: 25 μM of **1c** + DNA; Lane 7: 5 μM of **2c** + DNA; Lane 8: 10 μM of **2c** + DNA; Lane 9: 15 μM of **2c** + DNA; Lane 10: 20 μM of **2c** + DNA; Lane 11: 25 μM of **2c** + DNA; Lane 12: 5 μM of **3c** + DNA; Lane 13: 10 μM of **3c** + DNA; Lane 14: 15 μM of **3c** + DNA; Lane 15: 20 μM of **3c** + DNA; Lane 16: 25 μM of **3c** + DNA.

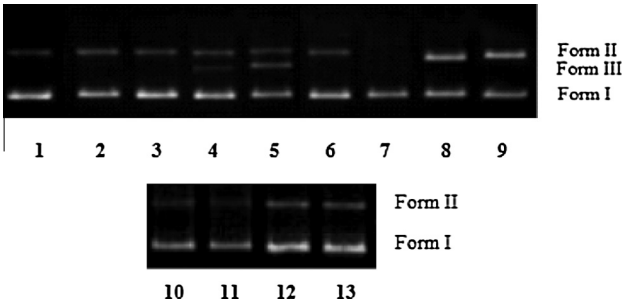


**Fig. 6.** Gel electrophoresis pattern for the cleavage pattern of pBR322 plasmid DNA (300 ng) by compounds (**1c–3c**) (25 mM) in the presence of ROS at 310 K after incubation for 1 h. Lane 1, DNA control; Lane 2, DNA + **1c** + DMSO (0.4 μM); Lane 3, DNA + **1c** + ethyl alcohol (0.4 μM); Lane 4, DNA + **1c** + $NaN_3$ (0.4 μM); Lane 5, DNA + **1c** + SOD (15 Units); Lane 6, DNA + **2c** + DMSO (0.4 μM); Lane 7, DNA + **2c** + ethyl alcohol (0.4 μM); Lane 8, DNA + **2c** + $NaN_3$ (0.4 μM); Lane 9, DNA + **2c** + SOD (15 Units). Lane 10, DNA + **3c** + DMSO (0.4 μM); Lane 11, DNA + **3c** + ethyl alcohol (0.4 μM); Lane 12, DNA + **3c** + $NaN_3$ (0.4 μM); Lane 13, DNA + **3c** + SOD (15 Units).

reflected by relaxation of the supercoiled circular form (Form I) of pBR322 DNA resulting in nicked circular (Form II) and/or linear form (Form III). The DNA cleavage ability of the compounds (**1c–3c**) was performed on pBR322 DNA (300 ng) incubated at 310 K with increasing concentration of compounds (5–25 μM) in aqueous buffer solution (5 mM Tris–HCl/50 mM NaCl, pH 7.2) for 1 h. As shown in Fig. 4, it was observed that all the compounds are found to exhibit nuclease activity at different concentration. The steroidal pyrans converted supercoiled DNA (Form I) into NC DNA (Form II) without concurrent formation of Form III suggesting single strand DNA cleavage (Lane 2–11). Compound **1c** showed efficient cleavage in comparison to **2c** and **3c**; with increase in concentration intensified nicked form (Form II) was observed.

### *3.2.4. DNA cleavage in presence of recognition elements (Groove binding agents)*

The potential interacting site of compounds (**1c–3c**) with pBR322 DNA were determined in presence of minor groove binding agent, DAPI and the major groove binding agent, methyl green (MG). The supercoiled pBR322 DNA was treated with DAPI or methyl green prior to the addition of compounds. The cleavage reaction mediated by compounds (**1c–3c**) was inhibited in presence of DAPI while it remained unaffected in the presence of MG (Fig. 5) indicating minor groove-binding preference of the compounds.

### *3.2.5. DNA cleavage in presence of reactive oxygen species (ROS)*

In order to explore the mechanistic pathway of the cleavage activity, comparative DNA cleavage experiment of compounds (**1c–3c**) were carried out in presence of some known radical scavengers such as DMSO and ethyl alcohol (EtOH) as hydroxyl radical scavenger (·OH), sodium azide ($NaN_3$) as singlet oxygen ($^1O_2$) quencher and superoxide dismutase (SOD) as superoxide anion radical ($O_2^{\cdot-}$) scavenger were used prior to the addition of compounds to DNA solution (Fig. 6). The addition of DMSO (Lane 2), EtOH (Lane 3) to compound **1c** diminishes the cleavage activity which is indicative of the involvement of hydroxyl radical in the cleavage process. In the case of $NaN_3$ and SOD (Lane 4 and 5), the Form II of plasmid DNA was converted to linear Form III indicating two subsequent and proximate single strand breaks of DNA non-randomly. Similarly, compound **2c** showed inhibition of DNA cleavage in presence of DMSO (Lane 6) whereas ethyl alcohol completely quench the formation of band II (Lane 7), suggestive of involvement of diffusible (·OH) hydroxyl radicals as one of the ROS responsible for DNA breakage. On the other hand, addition of $NaN_3$ and SOD did not show significant quenching of the cleavage revealing that singlet oxygen and superoxide anion were not involved in the cleavage process (Lane 8 and 9). The compound **3c** also showed inhibition of DNA cleavage in presence DMSO (Lane 10) while as ethyl alcohol also quench the formation of band II (Lane 11), revealing the fact (·OH) hydroxyl radicals being responsible for DNA breakage. Since, the compounds (**1c–3c**) are able to cleave DNA in the absence of any reducing agent, which reveal that DNA might be cleaved by a discernible hydrolytic pathway.

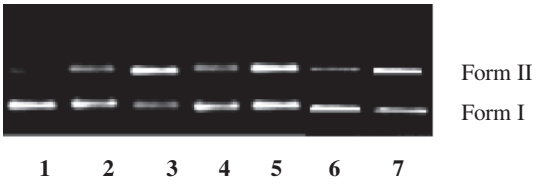


**Fig. 5.** Agarose gel electrophoresis pattern for the cleavage of pBR322 plasmid DNA (300 ng) by compounds (**1c–3c**) in the presence of DNA minor groove binding agent DAPI and major groove binding agent methyl green at 310 K after incubation for 30 min. Lane 1: DNA control; Lane 2: DNA + **1c** + DAPI (8 μM); Lane 3: DNA + **1c** + Methyl green (2.5 μL of a 0.01 mg $ml^{-1}$ solution); Lane 4: DNA + **2c** + DAPI (8 μM); Lane 5: DNA + **2c** + Methyl green (2.5 μL of a 0.01 mg $ml^{-1}$ solution); Lane 6: DNA + **3c** + DAPI (8 μM); Lane 7: DNA + **3c** + Methyl green (2.5 μL of a 0.01 mg $ml^{-1}$ solution).

### *3.2.6. Detection of hydroxyl radicals (·OH)*

In the DNA cleavage reactions mediated by various antioxidants in the presence of Cu (II), it has been established that Cu (II) is reduced to Cu (I) by the antioxidants and that Cu (I) is an essential intermediate in the DNA cleavage reactions [35,36]. It is also generally understood that DNA cleavage by various antioxidants and Cu (II) is the result of the generation of hydroxyl radicals. As mentioned in literature [37], Cu (II) is reduced to Cu (I) and the re-oxidation of Cu (I) to Cu (II) by molecular oxygen gives rise to superoxide anion which in turn leads to the formation of $H_2O_2$. Presumably Cu (I) is oxidized to Cu (II) by $H_2O_2$ in a Fenton type reaction giving rise to hydroxyl radicals (·OH). To determine the hydroxyl radical production and the role of copper ions in DNA cleavage, an experiment was performed where progressively increasing concentrations of compound **1c** and Cisplatin (12.5–600 μM) were tested on thiobarbituric acid induced DNA breakage (Fig. 7) and from these results we may conclude that the DNA cleavage by thiobarbituric acid involves endogenous copper ions (Cu (I) acts an intermediate) that leads to DNA cleavage. The

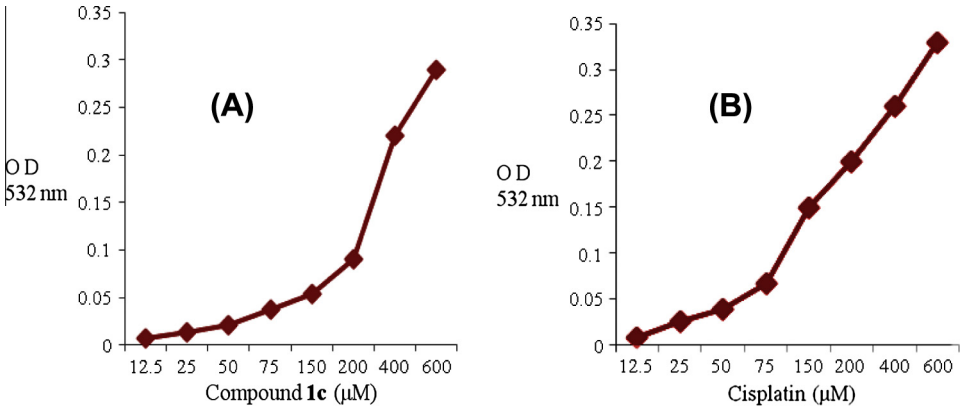


**Fig. 7.** Comperative determination of hydroxyl radical production by compound **1c** (A) and Cisplatin (B) by the assay of thiobarbituric acid.

compound **1c**-Cu (II) (Fig. 7A) and Cisplatin-Cu (II) (Fig. 7B) are shown to generate the hydroxyl radicals (·OH) which react with Calf thymus DNA, resulting in strand breaks. The assay is based on the fact that degradation of DNA by hydroxyl radical results in the release of TBA reactive material, which forms a colored adduct readable at 532 nm [38]. Increasing concentrations of compound **1c** or Cisplatin in presence of Cu (II) showed a corresponding increase in the generation of hydroxyl radicals. The results in Fig. 7 confirmed the relatively higher rate of formation of hydroxyl radicals and correlated with the rate of DNA degradation by the compound **1c** as well as Cisplatin.

### 3.2.7. T4 ligation experiment

To confirm the discernible hydrolytic DNA cleavage pathway mediated by compounds (**1c**–**3c**), DNA relegation experiment was performed in which supercoiled pBR322 DNA was treated with T4 ligase enzyme and subjected to gel electrophoresis [39]. Under our experimental conditions, the nicked form (Form II) was relegated to a large extent in the presence of T4 ligase enzyme in comparison to control DNA alone in supercoiled form (Fig. 8), providing a direct evidence in favor of hydrolytic mechanism.

### 3.2.8. Molecular docking

The design of molecules that can recognize specific sequences and structures of nucleic acids play an important role both for understanding nucleic acid molecular recognition as well as for the development of new chemotherapeutic drugs. Moreover molecular docking technique is an attractive scaffold to understand the Drug–DNA interactions for the rational drug design and discovery, as well as in the mechanistic study by placing a molecule into the binding site of the target specific region of the DNA mainly in a non-covalent fashion [40], which can substantiate the spectroscopic results.

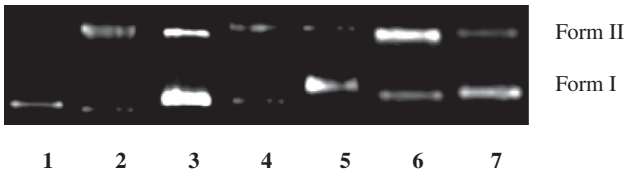


**Fig. 8.** Gel electrophoresis pattern for the ligation pBR322 plasmid DNA linearized by compounds (**1c**–**3c**); Lane 1, DNA control; Lane 2, pBR322 plasmid DNA cleaved by compound **1c**; Lane 3, ligation of nicked pBR322 plasmid DNA by T4 DNA ligase, Lane 4, pBR322 plasmid DNA cleaved by compound **2c**, Lane 5, ligation of nicked pBR322 plasmid DNA by T4 DNA ligase, Lane 6, pBR322 plasmid DNA cleaved by compound **3c**, Lane 7, ligation of nicked pBR322 plasmid DNA by T4 DNA ligase.

In our experiment, molecular docking studies of compounds **3a**–**3c** with DNA duplex of sequence d(CGCGAATTCGCG)$_2$ dodecamer (PDB ID: 1BNA) were performed in order to predict the chosen binding site along with preferred orientation of the molecules inside the DNA groove. The electrostatic interaction between the compounds and base pairs of DNA is mainly by hydrogen bonding shown by the $NH_2$ of the pyran ring. In the docked pose (Fig. 9a), $NH_2$ of the compound **1c** forms two hydrogen bonds with the base pairs of DNA; one hydrogen bond is with the 2nd oxygen of 15th cytosine of DNA while second hydrogen bond is with the 3rd oxygen of 16· guanine of DNA. In Fig. 9b, the oxygen of the pyran ring of compound **2c** forms one hydrogen bond with the first oxygen of 13th cytosine of DNA. In Fig. 9c, the $NH_2$ of the compound **3c** forms three hydrogen bonds with the base pairs of DNA; one hydrogen bond is with the 3rd oxygen of 15th cytosine of DNA; second with 5th oxygen of 16th guanidine of DNA while third hydrogen bond is with the 4th oxygen of 16th guanine of DNA.

Changes in accessible surface area of interacting residues show a preferential binding of compound between G-C base pairs and bends the DNA slightly in such a way that a part of the molecule comes between the two base pairs of the DNA helix which makes favorable stacking interactions between the ring systems of the DNA bases and the pyran ring of compound. The resulting binding energy of docked (steroid 4H-pyrans **1c**, **2c**, **3c** –DNA) complexes was found to be $-311.34$ kJ mol$^{-1}$, $-301.42$ kJ mol$^{-1}$ and $-308.61$ kJ mol$^{-1}$, respectively. The more negative the relative binding, the more potent is the binding between DNA and target molecule. Thus, we can conclude that there is a mutual complement between spectroscopic techniques and molecular docked model, which can be substantiate our spectroscopic results and at the same time provides further evidence of groove binding.

### 3.3. In vitro cytotoxicity

Some studies in recent past have showed that synthetic steroids with $\alpha$, $\beta$-unsaturated ketone core gave the potency against human cancer cell lines [41–43]. Thus with this interest, an attempt of synthesizing the steroidal 4*H*-pyran derivatives (**1c**–**3c**) from steroidal $\alpha$, $\beta$-unsaturated ketones (**1b**–**3b**) was made. Subsequently the compounds were evaluated for cytotoxicity against human cancer cell lines: SW480, A549, HepG2, HeLa, MCF-7, DU 145 and HL-60. The conversion of the soluble yellowish MTT to the insoluble purple formazan by active mitochondrial lactate dehydrogenase of living cells has been used to develop an assay system for measurement of cell proliferation.

The preliminary anticancer screening data given in Table 1 shows that compounds **1c**–**3c** exhibited different levels of cytotoxicity during which compound **1c** is found to have effective $IC_{50}$

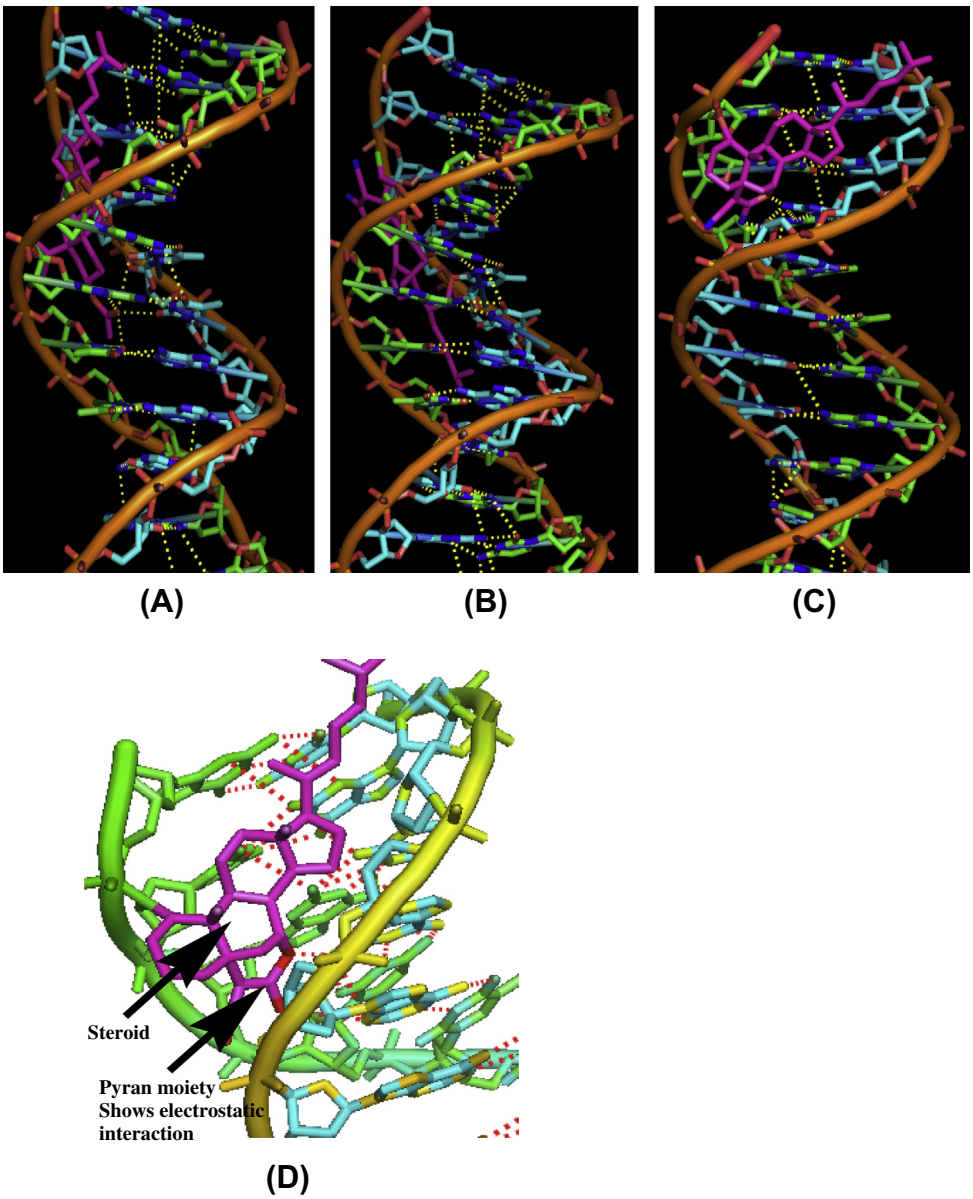


**Fig. 9.** Molecular docked models of steroidal pyrans (a) **1c**, (b) **2c**, (c) **3c** and (d) Docked pose showing the general intercalation of compounds with DNA dodecamer duplex of sequence d(CGCGAATTCGCG)$_2$ (PDB ID: 1BNA) and the yellow dashed lines showing hydrogen bond interaction. Steroidal 4H-pyrans are shown by the purple colour.

**Table 1**
Showing anticancer activity data of compounds (**1c**–**3c**) against cancer cell lines.

| Compound | $IC_{50}$ (μmol $L^{-1}$) | | | | | | |
|---|---|---|---|---|---|---|---|
| | Colon SW480 | Lung A549 | Hepatic HepG2 | Cervical HeLa | Breast MCF-7 | Prostate DU 145 | Leukaemia HL-60 |
| **1c** | 16.56 | 19.87 | 15.23 | 19.61 | 13.21 | 14.77 | 20.57 |
| **2c** | >50 | 26.46 | 25.72 | 36.80 | 33.17 | 41.48 | 35.61 |
| **3c** | 27.45 | 31.34 | >50 | 36.12 | 19.72 | 28.16 | >50 |
| Doxorubicin | 10.34 | 8.28 | 7.36 | 11.53 | 12.41 | 6.26 | 9.64 |
| Cisplatin | 3.52 | 12.1 | 9.63 | 9.43 | 9.3 | 6.54 | 7.83 |

values (<20 μmol $L^{-1}$) against given cancer cells; 13.21 μmol $L^{-1}$ (MCF-7), 14.77 μmol $L^{-1}$ (DU-145), 15.23 μmol $L^{-1}$ (HepG2), 16.56 μmol $L^{-1}$ (SW480) and 19.87 μmol $L^{-1}$ (A549). The compound **2c** is showing less cytotoxicity as its inhibition count ($IC_{50}$) values against given cancer cells is higher (>20 μmol $L^{-1}$); 26.46 μmol $L^{-1}$ (A549), 25.72 μmol $L^{-1}$ (HepG2), 36.80 μmol $L^{-1}$ (HeLa) and 33.17 μmol $L^{-1}$ (MCF-7). The compound **3c** is also showing higher $IC_{50}$ values against given cancer cells higher (>20 μmol $L^{-1}$), 27.45 μmol $L^{-1}$ (SW 480), 31.34 μmol $L^{-1}$ (A549), 36.12 μmol $L^{-1}$ (HeLa), 19.72 μmol $L^{-1}$ (MCF-7), 28.16 μmol $L^{-1}$ (DU 145). The compound **2c** and **3c** are almost inactive as they show $IC_{50}$ > 50 μmol $L^{-1}$ against SW480, HepG2 and HL-60 cells.

From the table it is clear that the compound **1c** was found to be potentially cytotoxic among all screened compounds and its $IC_{50}$ against MCF-7 was found to be 13.21 μmol $L^{-1}$ which is very close to the $IC_{50}$ of standard drug, Doxorubicin (12.41 μmol $L^{-1}$). Compound **1c** also showed potential cytotoxic behavior against DU-145, HepG2 and SW480 cells by showing $IC_{50}$ = 14.77 μmol $L^{-1}$, 15.23 μmol $L^{-1}$ and 16.56 μmol $L^{-1}$, respectively. Since compound **2c** and **3c** were not found so much potent as their inhibition was at higher concentration i.e.>25 μmol $L^{-1}$ against given cancer cells except MCF-7 cells against which compound **3c** expressed a moderate behavior by showing $IC_{50}$ = 19.72 μmol $L^{-1}$. During anticancer screening, none of the synthesized compounds were found as effective as the standard anticancer drugs like Doxorubicin, 5-Fluorouracil or Cisplatin, except compound **1c** which showed IC50 = 13.21 μmol $L^{-1}$ which is very close to the IC50 of 5-Fluorouracil (16.32 μmol $L^{-1}$) against MCF-7 cell line.

Microscopic examination of gross morphology of cancer cells and comparison with steroid 4H-pyran **1c**-treated normal and cancer cells is shown in Fig. 10. The growth of adenocarcinoma colon cells (SW480) (Fig. 10A) treated with 24 mM was inhibited within 24 h (Fig. 10B) but after 37 h cells were completely dead (Fig. 10C). The hepatic carcinoma cells (HepG2) (Fig. 10D) when treated with 24 mM also showed same behavior, the growth was inhibited within 24 h (Fig. 10E) but after 37 h cells were almost completely dead (Fig. 10F). The breast cancer cells (MCF-7) (Fig. 10G) and prostate cancer cells (DU-145) (Fig. 10J) also followed the same pattern of growth inhibition, as it is clear that after treatment for 24 h with steroidal pyran **1c**, the growth is inhibited in MCF-7 (Fig. 10H) and DU-145 (Fig. 10K) while as after 37 h treatment the MCF-7 (Fig. 10I) and DU-145 cells (Fig. 10L) were almost completely dead.

To confirm the cytotoxicity of steroidal pyrans, the compounds **(1c–3c)** were tested with some non-cancer cell lines NL-20 (lung)

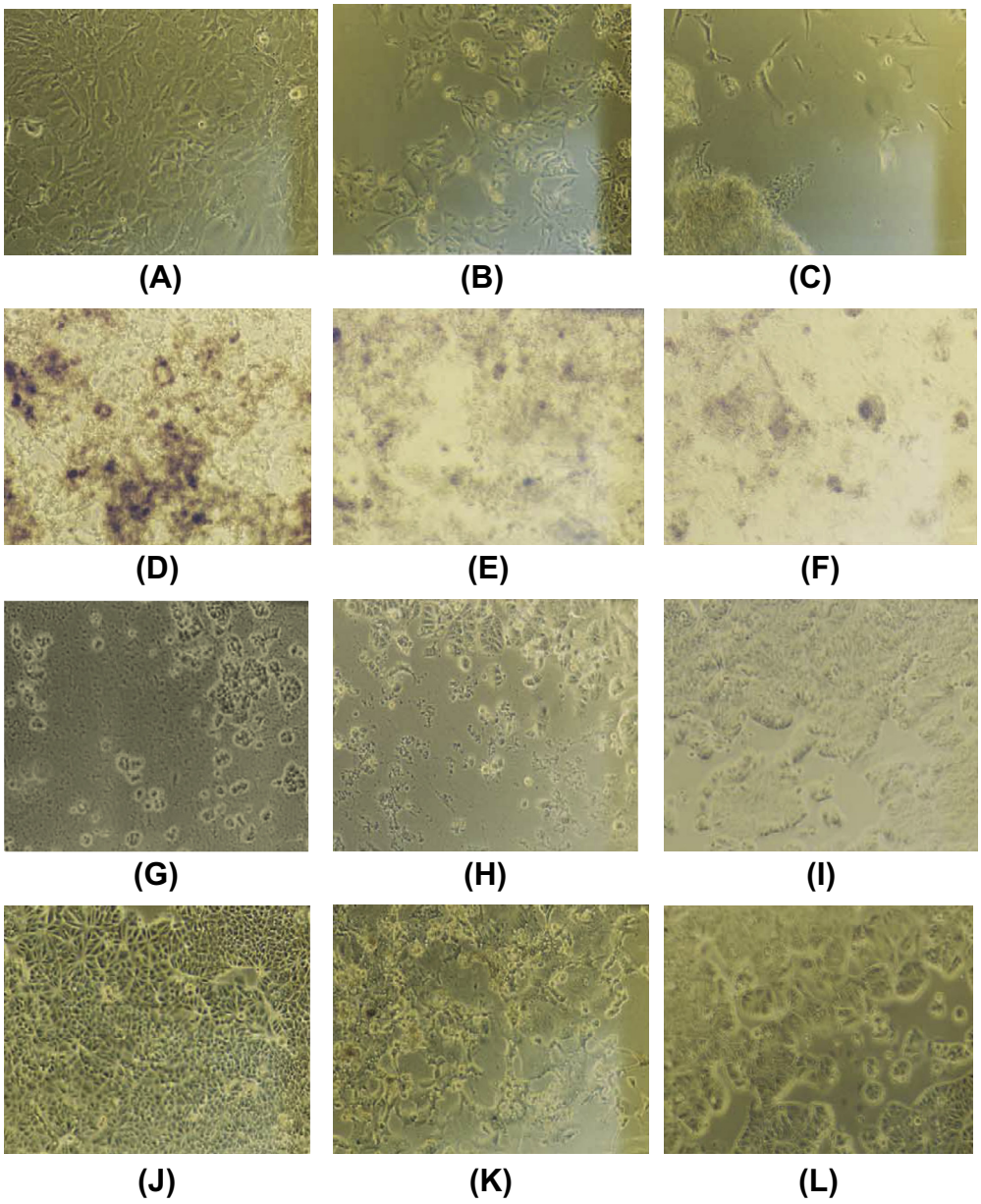


**Fig. 10.** Microscopic examination of the interaction of cancer cells with steroid pyran **1c**. (A), (B) and (C) represent SW480 control and cells treated with 24 mM of steroid pyran **1c** for 24 and 37 h, respectively. (D), (E) and (F) represent HepG2 control and cells treated with 24 mM of steroid pyran **1c** for 24 and 37 h, respectively. (G), (H) and (I) represent MCF-7 control and cells treated with 24 mM of steroid pyran **1c** for 24 and 37 h, respectively. (J), (K) and (L) represent DU-145 prostatic cancer cell control and cells that reacted with 24 mM of steroid pyran **1c** for 24 and 37 h, respectively.

**Table 2**
The $GI_{50}$ values shown by compound (**1c**–**3c**), Doxorubicin and Cisplatin against the non-cancerous cells.

| Compounds | $GI_{50}$ ($\mu M\ L^{-1}$) | | |
|---|---|---|---|
| | Lung NL-20 | Pulp HPC | Periodontal HPLF |
| **1c** | >100 | >100 | >100 |
| **2c** | >100 | >100 | 93.81 |
| **3c** | 80.58 | >100 | >100 |
| Doxorubicin | 91.77 | >100 | >100 |
| Cisplatin | 51.25 | 63.35 | 61.17 |

and HPC (pulp) during which none of the synthesized compounds were found toxic, all the compounds showed $GI_{50} > 55\ \mu mol\ L^{-1}$. This also suggests that the steroidal pyran derivatives can be used specifically for the treatment of cancer cells without showing toxicity to the non-cancer cells. The $GI_{50}$ which is the molar concentration causing 50% growth inhibition of non-cancerous cells by compounds **(1c–3c)** and Cisplatin are given in Table 2.

### 3.4. Comet assay (Single cell gel electrophoresis)

In the comet assay, the images of cells treated with Cisplatin and compounds (**1c**–**3c**) showed the formation of comets. No comet pattern was observed in the control cells (untreated). There was dose-dependent increase in tail length when treated with compounds (**1c**–**3c**) as shown in Fig. 11. Compound **1c** presented maximum apoptotic DNA damage among the three steroidal 4H-pyrans studied, which is in accordance with its maximum cytotoxicity as seen in MTT assay. None of the steroidal 4H-pyrans exhibited apoptotic DNA damage to the extent of Cisplatin. The quantified increase in DNA damage suggested that all three 4H-pyran derivatives induced dose dependent fragmentation of chromosomal DNA leading to apoptosis. The images of comet assay for control, cells treated with Cisplatin (0.1 μM, 54 μg/mL), **1c** (50 μg/mL), **2c** (50 μg/mL), and **3c** (50 μg/mL) are shown in Fig. 12. Slides were analyzed for parameter like tail length (TL),

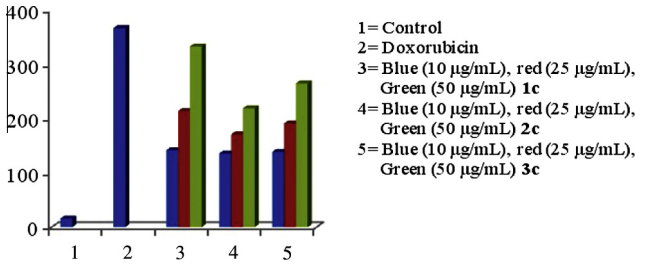


**Fig. 12.** Graph comparing the effect of steroidal pyrans on the tail length in comet assay. There was a concentration-dependent increase in the apoptotic DNA fragmentation and hence an increase in tail length in all three pyran derivatives. The extent of damage caused by Doxorubicin (0.1 μM) was more when compared to the three pyran derivatives (**1c**–**3c**). Compound **1c** caused maximum DNA damage in the comet assay.

using image analyzer CASP software version 1.2.2. The results of the assay for tail length are shown in Fig. 12.

## 4. Conclusion

We have developed a facile, convenient and efficient approach for the synthesis of new steroidal 4H-pyrans from steroidal α, β unsaturated ketones. Absorption and fluorescence studies reveal the stabilization of the energy levels of the compounds in presence of DNA. The molecular docking studies undertaken in the present work are in total agreement, with the primary intercalative mode of binding and the intercalation of compounds in between the nucleotide base pairs is due to the pyran moiety. The compounds bind to DNA preferentially through electrostatic and hydrophobic interactions. The gel electrophoresis demonstrated that the compound **1c** alone or in presence of Cu (II) causes the nicking of supercoiled pBR322 and follow the mechanistic pathway involving generation of hydroxyl radicals that are responsible for initiating DNA strand scission. From the *in vitro* cytotoxicity screening, it is clear that compound **1c** were found to be potential cytotoxic agent in comparison with standard drugs, Cisplatin and Doxorubicin. From the comet assay, it is also clear that the compound **1c** showed

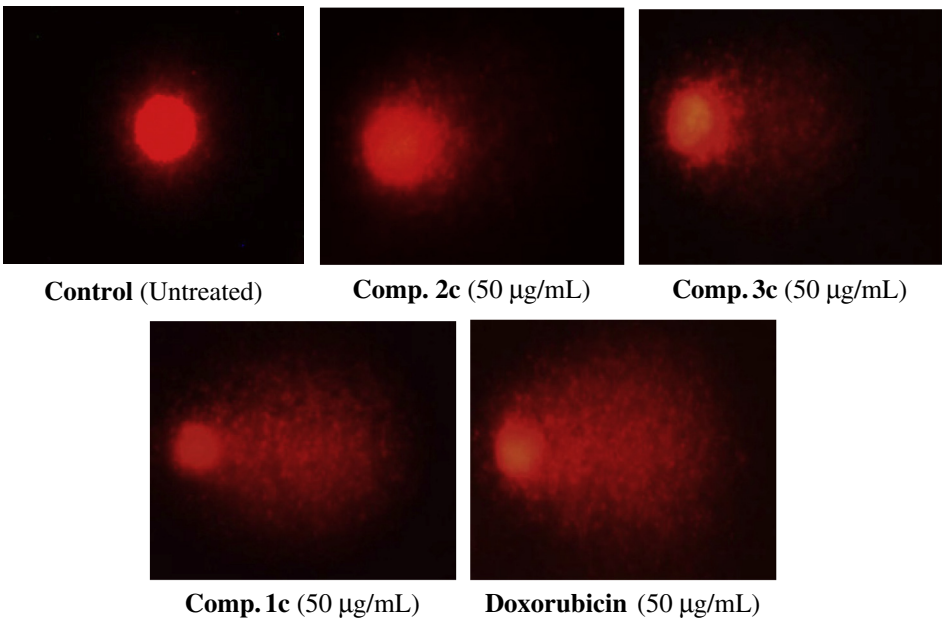


**Fig. 11.** Detection of DNA damage in MCF-7 cells. Treated cells (24 h) were layered over agarose gel, lysed, electrophoresed in alkaline buffer and stained with propidium iodide. Control cells were treated with DMSO alone. The DNA fragmentation resulting in a comet-like appearance in cells treated with Doxorubicin and compounds (**1c**–**3c**).

highest genotoxicity by showing the maximum tail length. In conclusion, the present study showed that the synthesized compounds can be used as template for future development through modification and derivatization to design more potent and selective cytotoxic agents.

## Acknowledgments

Authors thank the Chairman, Department of Chemistry, A.M.U., Aligarh, for providing necessary research facilities and the UGC for financial support in the form of research fellowship. Facilities provided by SAP (DRS-I) for their generous research support are also gratefully acknowledged. Authors also thank Department of Biochemistry, AMU, Aligarh and ICGEB, New Delhi for biological studies.

## References

[1] J.E. Cabaj, D. Kairys, T.R. Benson, Development of a commercial process to produce oxandrolone, Org. Process Res. Dev. 11 (2007) 378–388.
[2] S. Mennerick, Y. He, X. Jiang, B.D. Manion, M. Wang, A.A. Shute, A. Benz, A.S. Evers, D.F. Covey, C. Zorumski, Selective antagonism of 5α-reduced neurosteroid effects at GABA (A) receptors, Mol. Pharmacol. 65 (2004) 1191–1197.
[3] S.C. Kuo, L.J. Huang, H. Nakamura, Studies on heterocyclic compounds. 6. Synthesis and analgesic and anti-inflammatory activities of 3,4-dimethylpyrano[2,3-c]pyrazol-6-one derivatives, J. Med. Chem. 27 (1984) 539–544.
[4] V.Y. Sosnovskikh, M.A. Barabanov, B.I. Usachev, R.A. Irgashev, V.S. Moshkin, Synthesis and some properties of 6-di(tri) fluoromethyl- and 5-di(tri)fluoroacetyl-3-methyl-1-phenyl pyrano[2,3-c]pyrazol-4(1H)-ones, Russ. Chem. Bull. 54 (2005) 2846–2850.
[5] S. Hatakeyama, N. Ochi, H. Numata, S. Takano, A new route to substituted 3-methoxy carbonyl dihydropyrans; enantioselective synthesis of (−)-methyl elenolate, J. Chem. Soc., Chem. Commun. 17 (1988) 1202–1204.
[6] R.M. Burger, Cleavage of nucleic acids by bleomycin, Chem. Rev. 98 (1998) 1153–1169.
[7] (a) F.H. Westheimer, Why nature chose phosphates, Science 235 (1987) 1173–1178;
(b) D.S. Sigman, A. Mazumder, D.M. Perrin, Chemical nucleases, Chem. Rev. 93 (1993) 2295–2316.
[8] Y. Jin, J.A. Cowan, DNA cleavage by copper-ATCUN complexes. Factors influencing cleavage mechanism and linearization of dsDNA, J. Am. Chem. Soc. 127 (2005) 8408–8415.
[9] (a) J. Smith, K. Ariga, E.V. Anslyn, Enhanced imidazole-catalyzed RNA cleavage induced by a bis-alkyl guanidinium receptor, J. Am. Chem. Soc. 115 (1993) 362–364;
(b) J.R. Morrow, L.A. Buttrey, V.M. Shelton, K.A. Berback, Efficient catalytic cleavage of RNA by lanthanide (III) macrocyclic complexes: toward synthetic nucleases for in vivo applications, J. Am. Chem. Soc. 114 (1992) 1903–1905.
[10] U. Scheffer, A. Strick, V. Ludwig, S. Peter, E. Kalden, M.W. Gobel, Metal-free catalysts for the hydrolysis of RNA derived from guanidines, 2-aminopyridines, and 2-amino benzimidazoles, J. Am. Chem. Soc. 127 (2005) 2211–2217.
[11] Shamsuzzaman, H. Khanam, A. Mashrai, N. Siddiqui, Construction of novel steroidal isoxazolidinone derivatives under Vilsmeier-Haack conditions, Tetrahedron Lett. 54 (2013) 874–877.
[12] G.S. Son, Binding mode of norfloxacin to calf thymus DNA, J. Am. Chem. Soc. 120 (1998) 6451–6457.
[13] L.F. Fieser, M. Fieser, Steroids, vol. 28, Reinhold Publishing Corporation, New York, 1959.
[14] C.W. Shoppe, R.H. Jenkins, G.H.R. Summers, Steroids and Walden inversion. Part XXXIX. The halogenation of 5α-cholestan-6-one and the pyrolysis of 5-chloro-5α-cholestan-6-one, J. Chem. Soc. (1958) 1657–1663.
[15] W.G. Douben, K.H. Takemura, A study of the mechanism of conversion of acetate to cholesterol via Squalene, J. Am. Chem. Soc. 75 (1953) 6302–6304.
[16] M.E. Reicmann, S.A. Rice, C.A. Thomas, P. Doty, A furhter examination of the molecular weight and size of deoxy pentose nucleic acid, J. Am. Chem. Soc. 76 (1954) 3047–3053.
[17] A. Wolfe, G.H. Shimer, T. Meehan, Polycyclic aromatic hydrocarbons physically intercalate into duplex regions of denatured DNA, Biochemistry 26 (1987) 6392–6396.
[18] J.R. Lakowiez, G. Webber, Quenching of fluorescence by oxygen. A probe for structural fluctuations in macromolecules, Biochemistry 12 (1973) 4161–4170.
[19] S. Tabassum, M. Afzal, F. Arjmand, New heterobimetallic CuII-SnIV2 complex as potential topoisomerase I inhibitor: in vitro DNA binding, cleavage and cytotoxicity against human cancer cell lines, J. Photochem. Photobiol. B: Biol. 115 (2012) 63–72.
[20] G.J. Quinlan, J.M.C. Gutteridge, Oxygen radical damage to DNA by rifamycin SV and copper ions, Biochem. Pharmacol. 36 (1987) 3629–3633.
[21] X.Q. Chen, X. Peng, J. Wang, Y. Wang, S. Wu, L. Zhang, T. Wu, Y. Wu, Efficient increase of DNA cleavage activity of a Diiron (III) complex by a conjugating acridine group, Eur. J. Inorg. Chem. 42 (2007) 5400–5407.
[22] D. Mustard, D.W. Ritchie, Docking essential dynamics eigen structures, PROTEINS: Struct. Funct. Bioinf. 60 (2005) 269–274.
[23] W.L. Delano, The PyMOL Molecular Graphics System, DeLano Scientific, San Carlos, CA, USA, 2002.
[24] M. Chiba, M. Kimura, S. Asari, Exosomes secreted from human colorectal cancer cell lines contain mRNAs, microRNAs and natural antisen RNAs, that can transfer into the human hepatoma HepG2 and lung cancer A549 cell lines, Oncol. Rep. 28 (2012) 1551–1558.
[25] G. Shafi, A. Munshi, T.N. Hasan, A.A. Alshatwi, A. Jyothy, D.K.Y. Lei, Induction of apoptosis in HeLa cells by chloroform fraction of seed extracts of Nigella sativa, Cancer Cell Intern. 9 (2009) 29–36.
[26] A. Berenyi, R. Minorics, Z. Ivanyi, I. Ocsovszki, E. Duczaa, H. Thole, J. Messinger, J. Wolfling, G. Motyan, E. Mernyak, E. Frank, G. Schneider, I. Zupko, Synthesis and investigation of the anticancer effects of estrone-16-oxime ethers *in vitro*, Steroids 78 (2013) 69–78.
[27] X.-B. Wang, W. Liu, L. Yang, Q.-L. Guo, L.-Y. Kong, Investigation on the substitution effects of the flavonoids as potent anticancer agents: a structure–activity relationships study, Med. Chem. Res. 21 (2012) 1833–1849.
[28] T. Mosmann, Rapid colorimetric assay for cellular growth and survival: application to proliferation and cytotoxicity assays, J. Immunol. Methods 65 (1983) 55–63.
[29] H.O. Saxena, U. Faridi, J.K. Kumar, S. Luqman, M.P. Darokar, K. Shanker, C.S. Chanotiya, M.M. Gupta, A.S. Negi, Synthesis of chalcone derivatives on steroidal framework and their anticancer activities, Steroids 72 (2007) 892–900.
[30] H.J. Woerdenbag, T.A. Moskal, N. Pras, T.M. Malingre, F.S. El-Feraly, H.H. Kampinga, A.W. Konings, Cytotoxicity of artemisinin-related endoperoxides to ehrlich ascites tumor cells, J. Nat. Prod. 56 (1993) 849–856.
[31] C.V. Kavitha, M. Nambiar, C.S.A. Kumar, B. Choudhari, K. Muniyapa, K.S. Rangappa, S.C. Raghavan, Novel derivatives of spirohydantoin induce growth inhibition followed by apoptosis in leukemic cells, Biochem. Pharmacol. 77 (2009) 348–363.
[32] N.P. Singh, Microgels for estimation of DNA-strand breaks, DNA protein crosslinks and apoptosis, Mut. Res. 455 (2000) 111–127.
[33] N.A.A. El-Latif, A.E. Amr, A.A. Ibrahiem, Synthesis, reactions and pharmacological screening of heterocyclic derivatives using nicotinic acid as a natural synthon, Monatsh. Chemie 138 (2007) 559–567.
[34] N.S. Bhacca, D.H. Williams, Application of NMR Spectroscopy in Organic Chemistry, Holden Day, San Francisco, 1964. pp. 43–61.
[35] F.A. Shamsi, S. Husain, S.M. Hadi, DNA breakage by uric acid and Cu (II): binding of uric acid to DNA and biological, J. Biochem. Toxicol. 11 (1996) 67–71.
[36] M.S. Ahmad, F. Fazal, A. Rahman, S.M. Hadi, J.H. Parish, Activities of flavonoids for the cleavage of DNA in the presence of Cu(II): correlation with generation of active oxygen species, Carcinogenesis 13 (1992) 605–608.
[37] J.A. Badwey, M.L. Karnovsky, Active oxygen species and the functions of phagocytic leukocytes, Annu. Rev. Biochem. 49 (1980) 695–726.
[38] A. Gupte, R.J. Mumper, Elevated copper and oxidative stress in cancer cells as a target for cancer treatment, Cancer Treat. Rev. 35 (2009) 32–46.
[39] D. Mandal, M. Chauhan, F. Arjmand, G. Aromi, D. Ray, Interaction with DNA of a hetero nuclear [$Na_2Cu_4$] cordination cluster obtained from the assembly of two hydroxo-bridged [$CuI_2$] units by a dimeric sodium nitrate template, Dalton Trans. (2009) 9183–9191.
[40] R. Rohs, I. Bloch, H. Sklenar, Z. Shakked, Molecular flexibility in ab-initio drug docking to DNA: binding-site and binding-mode transitions in all-atom Monte Carlo simulations, Nucl. Acids Res. 33 (2005) 7048–7057.
[41] C. Li, W. Qiu, Z. Yang, J. Luo, F. Yang, M. Liu, J. Xie, J. Tang, Stereoselective synthesis of some methyl-substituted steroid hormones and their in vitro cytotoxic activity against human gastric cancer cell line MGC-803, Steroids 75 (2010) 859–869.
[42] C. Wang, L. Liu, H. Xu, Z. Zhang, X. Wang, H. Liu, Novel and efficient synthesis of 22-alkynyl-13, 24(23)-cyclo-18, 21-dinorchol-22-en-20(23)-one analogues, Steroids 76 (2011) 491–496.
[43] J.G. Cui, L. Fan, L. Huang, H. Liu, A. Zhou, Synthesis and evaluation of some steroidal oximes as cytotoxic agents: structure/activity studies (I), Steroids 74 (2009) 62–72.